New Soluble n-Type Conjugated Polymers for Use as Electron Transport Materials in Light-Emitting Diodes

Christopher J. Tonzola,[†] Maksudul M. Alam,[‡] Bryan A. Bean,[‡] and Samson A. Jenekhe*,[†,‡]

Department of Chemical Engineering and Department of Chemistry, University of Washington, Seattle, Washington 98195-1750

Received December 21, 2003; Revised Manuscript Received February 11, 2004

ABSTRACT: We report the synthesis of a series of six new soluble n-type conjugated copolymers that incorporate bis(phenylquinoline) and regioregular dialkylbithiophene in the backbone, the investigation of their electrochemical, photophysical, and electroluminescent properties, and their use as electron transport materials in light-emitting devices. Variation of the alkyl chain length of the head-to-head dialkylbithiophene linkage from butyl (C_4) to dodecyl (C_{12}) had little or no effect on the photophysical or redox properties of the new polyquinolines. However, the glass transition temperature decreased from 256 °C for the butyl derivative to 76 °C for the dodecyl derivative. A single-crystal X-ray structure of a model compound allowed quantification of the intramolecular torsion angles which explain the significant difference in optical band gap and redox properties between the head-to-tail and head-to-head polymers. The high electron affinity (2.88−2.97 eV), robust thermal stability, suitable solution processability, and weak-to-moderate intrinsic electroluminescence of the polymers make them attractive for use as electron transport materials in organic LEDs. Initial use of the polymers as the electron transport materials in bilayer poly(2-methoxy-5-(2′-ethylhexyloxy)-1,4-phenylenevinylene) (MEH−PPV) LEDs showed substantial enhancement in device performance under ambient air conditions (1.4% external quantum efficiency, 2170 cd/m^2) compared to most current electron transport polymers for LEDs.

Introduction

Emerging major applications of conjugated polymer semiconductors in polymer electronics and optoelectronics include light-emitting diodes (LEDs),[1−3] photovoltaic cells,[4] and thin film transistors.[5] One of the current broad needs in the field is the development of n-type (electron transport) conjugated polymer semiconductors for improving the performance of LEDs, solar cells, and n-channel thin film transistors. Electron injection and transport requirements for LEDs are sufficiently different from those for photovoltaic cells and thin film transistors.[1−5] Our paper is focused here on new electron transport materials for organic LEDs.

Most of the current highly fluorescent conjugated polymers used as emissive materials in LEDs, such as the numerous arylenevinylene polymers, polyfluorenes, and perhaps also polythiophenes, are good p-type (hole transport) materials.[1−3] They, however, have generally small electron affinities and poor electron transport properties. The use of electron-deficient heterocyclic small molecules or polymers as a separate electron transport layer or as a blend component in conjunction with the emissive material has proven very useful in improving balanced injection and recombination in organic LEDs.[1−3,6−11] Molecules and polymers containing oxadiazole,[6,7] benzothiadiazole,[8] benzobisazole,[9] quinoline,[10] quinoxaline,[11] and anthrazoline[10a] are some of the electron transport materials that have been explored for LED applications. Thermally robust conjugated poly(phenylquinoline)s,[12] which are known to have excellent photochemical stability even under high-intensity laser irradiation,[13] are particularly attractive for LED applications if their solubility in organic solvents can be achieved without compromise of thermal stability. Recent synthetic work has focused on development of organic solvent soluble fully conjugated polyquinolines for LED and other optoelectronic applications.[14]

In this paper we report the synthesis, characterization, and properties of a series of five new soluble, head-to-head (HH) regioregular, poly(2,2′-(3,3′-dialkyl-2,2′-bithienylene)-6,6′-bis(4-phenylquinolines)) (PxBTQ) in which the alkyl chain length is varied from butyl to dodecyl. In addition, a related new head-to-tail (HT) regioregular copolymer, poly(2,2′-(3,4′-dihexyl-2,2′-bithienylene)-6,6′-bis(4-phenylquinoline)) (HT-P6BTQ), was synthesized, characterized, and similarly investigated. The X-ray single-crystal structure of the HH model compound was obtained and used to explore structure−property relationships in the new polymers. All six new n-type polymers were investigated as electron transport materials in bilayer LEDs based on poly(2-methoxy-5-(2′-ethylhexyloxy)-1,4-phenylenevinylene) (MEH−PPV) as the emissive material. In a previous Communication, preliminary results were reported for one of the present polymers: poly(2,2′-(3,3′-dioctyl-2,2′-bithienylene)-6,6′-bis(4-phenylenequinoline)) (P8BTQ or POBTPQ).[14a] Furthermore, the morphology and energy transfer properties of binary blends of POBTPQ with MEH−PPV or poly(3-octylthiophene) (POT) were also reported.[10d]

Results and Discussion

Synthesis and Characterization. Scheme 1 outlines the synthesis of new monomers **2a**−**2e** and **4** through acetylation of dialkylbithiophenes. The dialkylbithiophenes **1** and **3** were synthesized according to literature methods.[15] The diacetyldialkylbithiophenes **2a**−**2e** and **4** were purified using column chromatography and recovered as amber oils with yields ranging from 33 to 49%. As shown in Scheme 2, diacetyl

[†] Department of Chemical Engineering.
[‡] Department of Chemistry.

10.1021/ma035971o CCC: $27.50
Published on Web 04/20/2004

Scheme 1. Synthesis of Monomers 2a−2e and 4

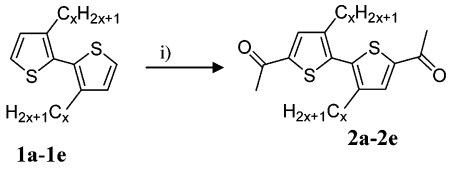

1a-1e **2a-2e**

x = 4 (**a**), 6 (**b**), 8 (**c**), 10 (**d**), 12 (**e**)

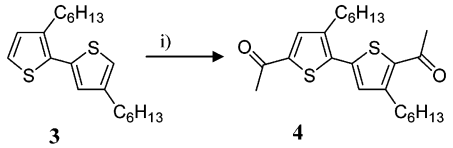

3 **4**

i) 2.2 eq. acetic anhydride, 2.2 eq. $SnCl_4$, anhyd. CH_2Cl_2, reflux, 24 h.

Scheme 2. Synthesis of New Polyquinolines

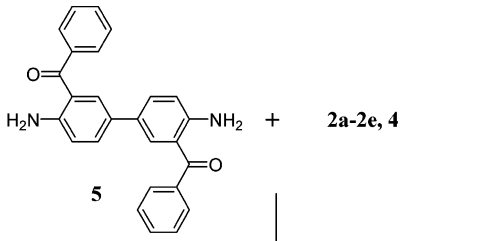

5

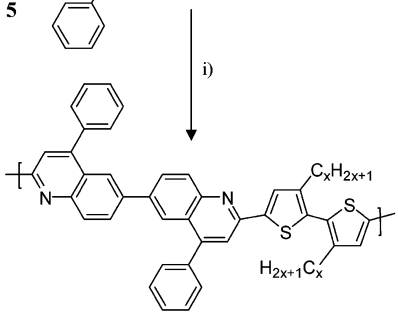

PxBTQ

x = 4 (**P4BTQ**), 6 (**P6BTQ**), 8 (**P8BTQ**), 10 (**P10BTQ**), 12 (**P12BTQ**)

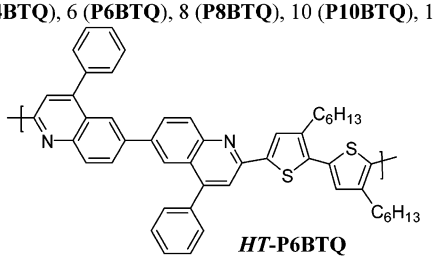

***HT*-P6BTQ**

i) diphenylphosphate, *m*-cresol, 140 °C, 72 h.

monomers **2a**−**2e** were then copolymerized with the (*o*-amino keto)-functionalized 3,3′-dibenzoylbenzidine (**5**)[16] to yield the polyquinolines that contained head-to-head regioregular bithiophenes (PxBTQ). Monomers **4** and **5** yielded the head-to-tail polymer HT-P6BTQ. The resulting polymers were precipitated into 10% triethylamine/ethanol and extracted on a Soxhlet apparatus with 20% triethylamine/ethanol for 2 days to remove the diphenyl phosphate (DPP) acid catalyst.[12] The polymers were obtained as either reddish-brown powders or fibrous materials. ^{1}H NMR and FT-IR spectra on all products confirmed the proposed structures. Thermogravimetric analysis (TGA) also indicated high purity with <2% weight loss at the decomposition temperatures (T_D). Elemental analysis of the polymers showed significant deviations from the theoretical values for carbon. This is, however, consistent with previous reports of polyquinolines and other high-temperature polymers. The origin of this discrepancy is incomplete combustion of the thermally stable polymers. The model compound BPQ-10BT was similarly synthesized using the Friedländer condensation reaction (Scheme 3). 5,5′-Diacetyl-3,3′-didecyl-2,2′-bithiophene was reacted with an excess of 2-aminobenzophenone to afford the model compound. BPQ-10BT was recrystallized twice in 4:1 THF/methanol mixture and was obtained as yellow crystals.

The weight-average molecular weights (M_w) based on polystyrene standards and gel permeation chromatography (GPC) are shown in Table 1. The M_w values are from 19 450 to 149 900. The wide range of the molecular weights of the series of polymers is due to difficulties in precisely controlling the stoichiometry of the comonomers, one which was a viscous oil. Polydispersities were in the range 1.89−2.88 with the exception of P10BTQ. This latter polymer showed the unusually high polydispersity of 6.20, which is likely a result of difficulties in controlling the polymerization temperature.

Thermal properties of all polymers are shown in Table 1. The decomposition temperatures (T_D) of the polymers were in the range 415−468 °C. Poly(phenylquinoline)s typically have glass transitions (T_g) between 200 and 400 °C.[17] We were able to determine the T_g of the polymers by differential scanning calorimetry (DSC) and further used modulated DSC (MDSC) to confirm the subtle glass transitions that were observed in some of the polymers. The T_g was between 161 and 256 °C for all polymers except the dodecyl-substituted P12BTQ, which had a T_g of 76 °C. The T_g was seen to decrease with increasing alkyl chain length. Typical second heating DSC curves for P6BTQ and HT-P6BTQ are shown in Figure 1. This comparison of both hexyl-substituted polymers indicated that the head-to-tail regioregularity of HT-P6BTQ resulted in a significantly lower T_g, 196 °C vs 247 °C for the head-to-head polymer. These results are in accord with the high thermal stability (T_g > 150 °C) associated with polyquinolines, with the obvious exception of P12BTQ.

Crystal Structure of Model Compound. The X-ray single-crystal structure of BPQ-10BT was obtained and studied to elucidate structure−property relationships in the polymers. Single-crystal structures of oligophenylquinolines have similarly provided valuable information as model systems for the conjugated poly(phenylquinoline)s.[18] Structure−property relationships from single-crystal structures also proved invaluable in recent work on related diphenylanthrazoline molecular semiconductors, where correlations between X-ray-determined structural characteristics and photophysical and electron transport properties were observed.[19]

Crystals of BPQ-10BT were grown by slow evaporation of a THF/methanol solution at 0 °C. The low melting point of BPQ-10BT (22 °C) required crystal growth to be done at the low temperature. BPQ-10BT has a primitive monoclinic crystal system with the unit cell parameters a = 17.4640 (9) Å, b = 9.4710 (5) Å, c = 29.8230 (19) Å, and β = 104.153 (2)°. The space group was $P2_1/c$. The structure was refined to final residual of R_1 = 6.65% for BPQ-10BT**.** The detailed crystallographic data for BPQ-10BT are provided in the Supporting Information.

The single-crystal structure and packing diagram are shown in Figure 2. The steric interaction between the alkyl chains and the sulfur atoms of the bithiophene is clearly evident by the large intramolecular torsion angle

Scheme 3. Synthesis of Model Compound

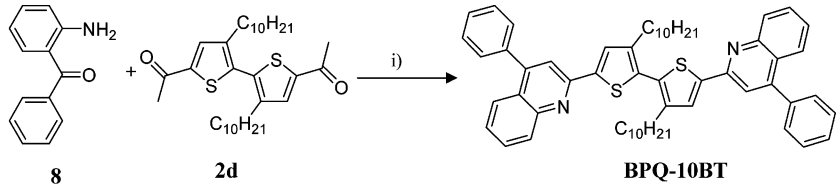

8 **2d** **BPQ-10BT**

i) diphenylphosphate, toluene, 140 °C, 24 h.

Table 1. Physical Properties of New Polyquinolines and Model Compound

cmpd	M_w (10^4)	PDI	T_D (°C)	T_g (°C)	λ_{max}^{abs} (soln) (nm)	ϵ (10^4 M^{-1} cm^{-1})	λ_{max}^{abs} (film) (nm)	E_g^{opt} (eV)	λ_{max}^{em} (soln) (nm)	λ_{max}^{em} (film) (nm)	ϕ_f (soln)	ϕ_f (film)
P4BTQ	3.9	2.88	445	256	410	8.1	424	2.44	502	524	0.22	0.01
P6BTQ	14.9	2.45	423	247	410	4.7	425	2.44	502	518	0.23	0.04
P8BTQ	6.5	2.71	439	190	411	5.7	419	2.44	503	523	0.27	0.03
P10BTQ	14.7	6.20	428	161	413	3.8	423	2.44	504	517	0.26	0.01
P12BTQ	1.9	1.95	415	76	408	6.6	416	2.44	502	523	0.28	0.03
HT-P6BTQ	1.9	1.89	468	196	444	4.9	462	2.24	508	562	0.26	0.01
BPQ-10BT	n/a	n/a	458	n/a	368	4.6	373	2.62	473	486	n/a	n/a

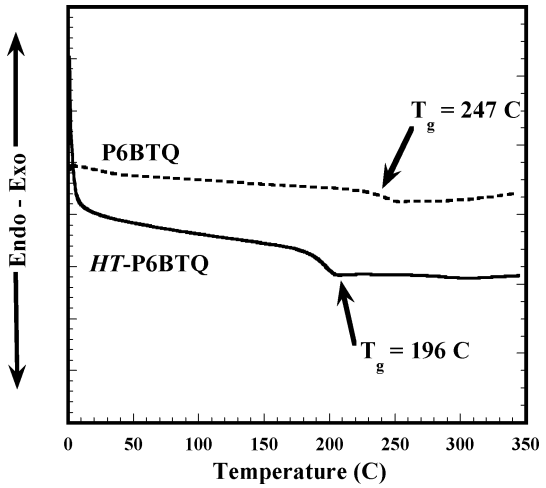

Figure 1. Second heating DSC curves of P6BTQ and HT-P6BTQ (10 °C/min).

between the thiophene units. The neighboring thiophenes are twisted by a 45° angle. In contrast, the phenyl rings in a oligoquinoline with a biphenylene linkage are coplanar.[18] The torsion angle between the thiophene and quinoline moieties in BPQ-10BT is only 21° and is likely due to the electronic interaction between the unpaired electrons on the nitrogen and sulfur atoms that lie in the plane of the molecule. The phenyl groups attached to the quinoline moiety are twisted 49°, which is in good agreement with previous crystal structures of oligophenylquinolines.[18]

Figure 2b shows the molecular packing of BPQ-10BT. It is evident that there is no π stacking, with distances between neighboring aromatic rings >8 Å. It seems that the decyl chains align themselves along the face of the aromatic rings of the neighboring molecules. This lack of order is significantly different than that observed in previous oligophenylquinolines.[18] Previous oligomers showed either face-to-face or edge-to-face π stacking. In both cases the distance between interacting aromatic rings is less than 4 Å. This provides evidence for the lack of strong intermolecular interactions in the present BPQ-10BT model compound and the related PxBTQ polymers.

Electrochemical Properties. Cyclic voltammetry was performed on films of all polymers. Typical cyclic voltammograms (CVs) are shown in Figure 3 for P6BTQ and HT-P6BTQ. These CV scans in the −2.2 to 1.6 V (vs SCE) range show quasi-reversible reduction peaks and irreversible oxidation peaks. Similar CVs were observed with the other PxBTQs. The redox CVs observed in the present series of polymers are very similar to those previously reported for other polyquinolines.[14a,b,20] We note that quasi-reversible oxidation was observed previously in bithiophene- and phenothiazine-linked polyquinolines,[20,21] with the latter being recently utilized in electrochromic devices.[22]

Table 2 shows the electrochemical data for all the new polymers. The formal reduction potential ($E_{red}^{o\prime} = (E_{pa} + E_{pc})/2$) varied from −1.80 V (vs SCE) for P4BTQ to −1.65 V for HT-P6BTQ. The onset reduction potential of HT-P6BTQ was also the most positive (−1.43 V) among the series of polyquinolines (Table 2). Electron affinities (LUMO levels) were estimated from these onset reduction potentials by using −4.4 eV as the SCE energy level relative to vacuum.[20,23] All six polyquinolines have electron affinities between 2.88 and 2.97 eV. Since the reduction potentials and LUMO levels of the polymers are relatively unchanged by the alkyl chain length or the regioregularity of the bithiophene linkage, we conclude that the LUMO levels of the polymers lie on the π^* orbital of the bis(quinoline) moiety.

The peak oxidation potential was relatively constant among the six polymers, being 1.39−1.45 V (vs SCE) as seen in Table 2. However, the variation of the onset oxidation potential from 0.82 V for HT-P6BTQ to 1.15 V for P10BTQ indicates that regioregularity of the bialkylbithiophene linkage has a significant consequence for redox properties. The ionization potentials (IP, HOMO levels) estimated relative to an SCE energy level of 4.4 eV were between 5.44 and 5.55 eV for PxBTQs whereas it was 5.23 eV for HT-P6BTQ. The decrease of ~0.25 eV in the ionization potential of HT-P6BTQ, compared to the other polymers, is indicative of the HOMO lying on the bithiophene moiety and thus can be modulated by the torsion angle between the thiophene rings. The electrochemically derived band gaps (E_g^{el}) of the series of polyquinolines are shown in Table 2. The band gap varies only slightly, 2.50−2.65 eV, among the HH-bithiophene-linked polymers. However, E_g^{el} is reduced to 2.25 eV in HT-P6BTQ.

Photophysical Properties. Absorption spectra of all six polymers in THF solution are shown in Figure 4a. The lowest energy absorption bands are from the $\pi-\pi^*$

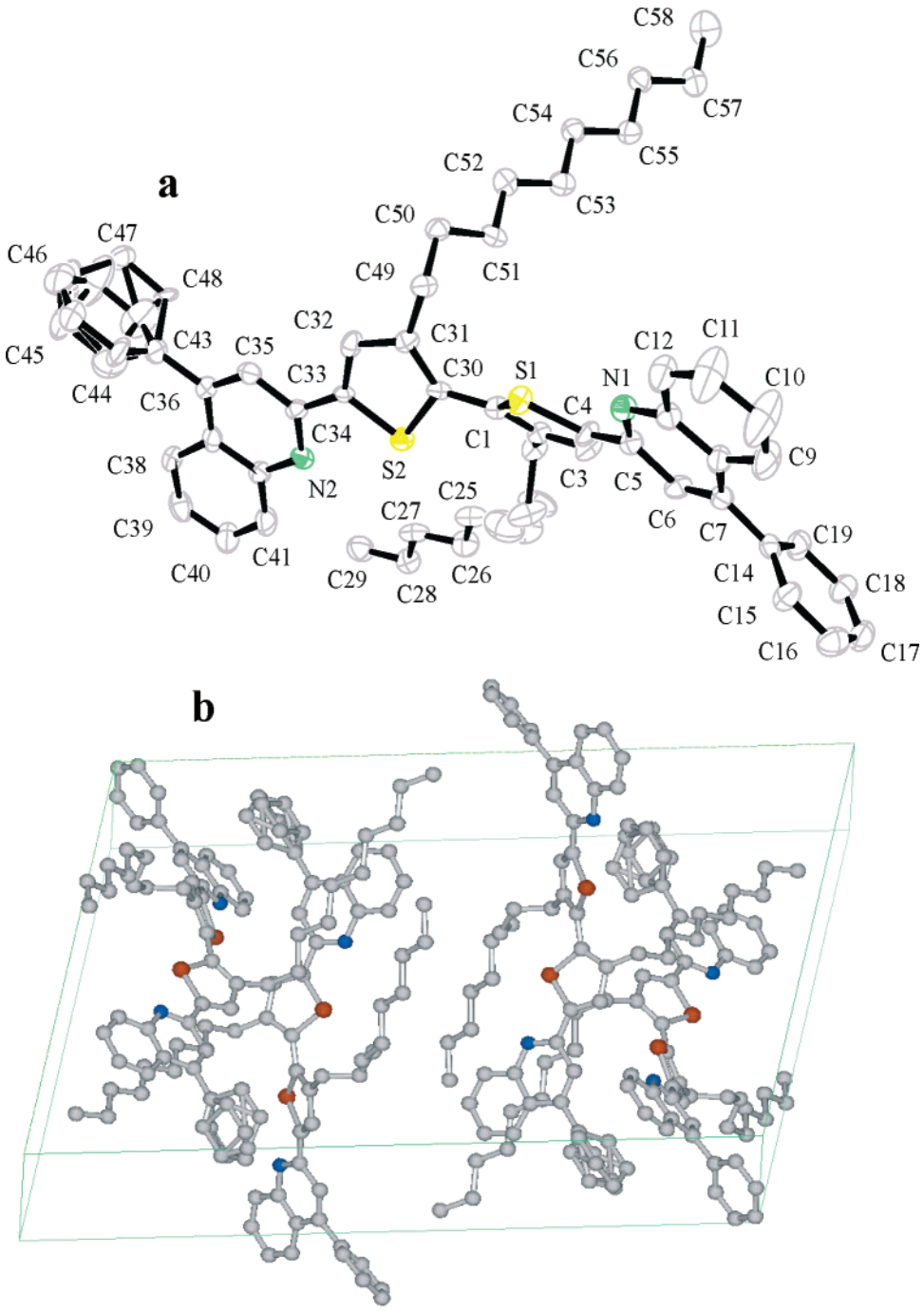

Figure 2. Single-crystal structure (a) and molecular packing (b) of model compound BPQ-10BT.

transitions by virtue of their large molar extinction coefficients ($\epsilon > 10^4$ M^{-1} cm^{-1}). All the solution absorption spectra of the polymers are structureless. The HH-bithiophene-linked PxBTQ have nearly identical absorption maxima (λ_{max}) between 408 and 413 nm. There is no evident trend for this slight difference in absorption spectra and maxima, and no correlation can be made between absorption maxima and molecular weight, polydispersity, or alkyl chain length. HT-P6BTQ, which contains the head-to-tail dihexylbithiophene linkage, has an absorption ($\lambda_{max} = 444$ nm) that is ~30 nm red-shifted compared to the HH-bithiophene-linked PxBTQ. This red shift is a result of the larger delocalization length in HT-P6BTQ due to the increased planarity of the bithiophene group. The steric interaction between the alkyl chain and the sulfur atom in the head-to-head bithiophene-linked polymers clearly leads to a large torsion angle and decrease in conjugation length compared to HT-P6BTQ.

The thin film optical absorption spectra of the polymers are shown in Figure 4b. The structureless absorption bands observed in solution are also seen in the solid state. The solid-state absorption bands are, however, red-shifted by between 7 and 18 nm, compared to their corresponding ones in solution. The similarity of the solution and the solid-state absorption spectral line shape in these macromolecules suggest that there is a slight increase in conjugation length in the solid state, accounting for the 7−18 nm red shift in absorption maximum. This slight red shift is a result of the increased planarity of the polymer in the solid state. The absorption λ_{max} was 416−424 nm for the PxBTQs and 462 nm for HT-P6BTQ. The latter λ_{max} value is to be compared to a λ_{max} of 468 nm previously reported

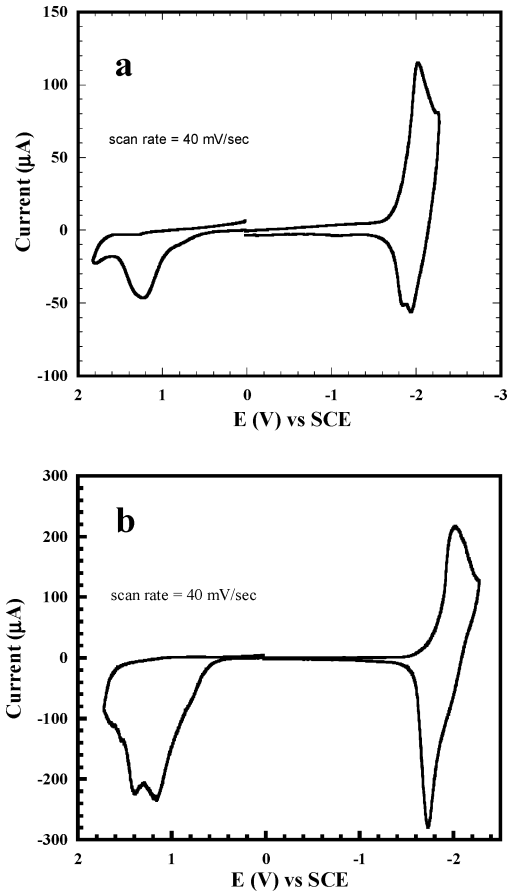

Figure 3. Cyclic voltammograms of thin films of P6BTQ (a) and HT-P6BTQ (b) on Pt electrode (0.1 M TBAF6 in MeCN).

for a bithiophene-linked polyquinoline (PBTPQ) with no alkyl chains on the bithiophene linkage.[12a,b] The similarity of the absorption λ_{max} of these two related polymers indicates that the alkyl chains of HT-P6BTQ provide minimal steric interaction with the polymer backbone. Optical band gaps (E_g^{opt}) determined from the absorption edge of the thin film spectra are given in Table 1. The optical band gap is 2.44 eV for all the PxBTQ except HT-P6BTQ, which has an E_g^{opt} of 2.24 eV. These values are in good agreement with those determined from cyclic voltammetry (Table 2).

The dilute solution (10^{-5} M) photoluminescence (PL) spectra of the polymers are shown in Figure 5a. All six polymers have slightly structured emission bands with emission maximum of 502−508 nm. The PL quantum yield (ϕ_f) of the polymers in dilute solution in THF was 22−28% (Table 1). These results show that there is little or no effect of the alkyl chain length on the solution luminescence of the polymers. A major reason for the low emission quantum yield of the series of polymers is their donor−acceptor nature and the consequent intramolecular charge transfer which is known to be an important luminescence quenching mechanism in such donor−acceptor systems.[21]

The PL emission spectra of the thin films are shown in Figure 5b. The line shape of the PL spectra is identical to that of the solution spectra. However, the solid-state emission bands are red-shifted from the dilute solution ones by 13−22 nm except HT-P6BTQ, whose PL spectrum is red-shifted by 54 nm compared to the dilute solution. We rule out intermolecular excimers[24] as important species in the solid-state emission of all the PxBTQs except in the HT-dihexylthiophene-linked polymer (HT-P6BTQ). The large red shift of the thin film PL emission spectrum of HT-P6BTQ compared to the dilute solution and the broad structureless line shape suggest excimer emission.[24] The PL quantum yields of the polymers in the solid state were low, 1−4% (Table 1). The especially poor PL emission efficiency in thin films is also in accord with the strong intramolecular charge-transfer character in the donor−acceptor polymers.[21]

Electroluminescence and Electron Transport Properties. We investigated the intrinsic electroluminescence (EL) of these compounds by using poly(ethylenedioxythiophene)/poly(styrenesulfonic acid) (PEDOT) thin film on indium tin oxide (ITO) as the anode, the spin-coated polyquinoline as the emissive layer, and aluminum as the cathode: ITO/PEDOT/PxBTQ/Al. The film thicknesses of the emissive polymers were approximately 75 nm. Representative EL spectra of the series of polymers are shown in Figure 6 for P6BTQ and HT-P6BTQ. The EL spectra are similar to the PL spectra (Figure 5b) to within 7−16 nm. In the case of HT-P6BTQ, the EL emission maximum was identical to the PL emission maximum. The device characteristics of the LEDs are shown in Table 3, and the corresponding current−voltage and luminance−voltage curves are shown in parts a and b of Figure 7, respectively. The turn-on voltage (electric field) of these diodes was 9−10 V (∼1.2×10^6 V/cm). The maximum brightness of the devices was only 16−64 cd/m^2, and the external quantum efficiency (EQE) was also low, 0.004−0.015% (Table 3). The poor device efficiency and brightness are a result of both the poor fluorescence quantum yields in thin films and the large barrier to hole injection of the n-type polymers. Clearly, these polymers are not very promising emissive materials but are more suited to the role of electron transport materials in LEDs.

The solubility of these new n-type polymers in formic acid provides the opportunity to fabricate bilayer LEDs by spin-coating over organic-solvent soluble polymers such as MEH−PPV. While the polyquinolines provide only a small minimization of the barrier to electron injection from the Al cathode compared to MEH−PPV, which has an electron affinity of 2.9 eV, the electron transport property of the n-type layer is primarily responsible for the improved performance. The significant enhancements in LED performance are a function of balanced charge recombination occurring away from the cathode.[14a,b] We thus fabricated bilayer LEDs ITO/PEDOT/MEH−PPV/PxBTQ/Al by spin-coating of the MEH−PPV layer from $CHCl_3$ followed by spin-coating of the polyquinolines from formic acid. The film thickness of the polyquinolines as electron transport layers in these diodes was in the range 55−60 nm. The EL spectra of the bilayer LEDs ITO/PEDOT/MEH−PPV/P6BTQ/Al and ITO/PEDOT/MEH−PPV/HT-P6BTQ/Al are shown in parts a and b of Figure 8, respectively. At all applied bias voltages in these and other bilayer diodes, only the characteristic orange-red emission of MEH−PPV with an EL emission maximum at 569 nm was seen, demonstrating that the polyquinolines functioned as electron transport materials.

The current−voltage and luminance−voltage characteristics of the MEH−PPV diodes using the new polyquinolines as electron transport materials are shown in Figure 9. The turn-on voltage (electric field) of these LEDs was about 9 V (∼9×10^5 V/cm). The maximum brightness of the LEDs was in the range of 948 cd/m^2

Table 2. Electrochemical Data for All New Polyquinolines[a]

cmpd	$E_{red}^{o'}$ (V)	E_{red}^{onset} (V)	EA (eV)	E_{ox}^{peak} (V)	E_{ox}^{onset} (V)	IP (eV)	E_g^{el} (eV)
P4BTQ	−1.80	−1.52	2.88	1.45	1.13	5.53	2.65
P6BTQ	−1.77	−1.46	2.94	1.45	1.04	5.44	2.50
P8BTQ	−1.76	−1.48	2.92	1.43	1.08	5.48	2.56
P10BTQ	−1.76	−1.50	2.90	1.52	1.15	5.55	2.65
P12BTQ	−1.71	−1.46	2.94	1.48	1.12	5.52	2.58
HT-P6BTQ	−1.65	−1.43	2.97	1.39	0.82	5.22	2.25

[a] All potentials are vs SCE.

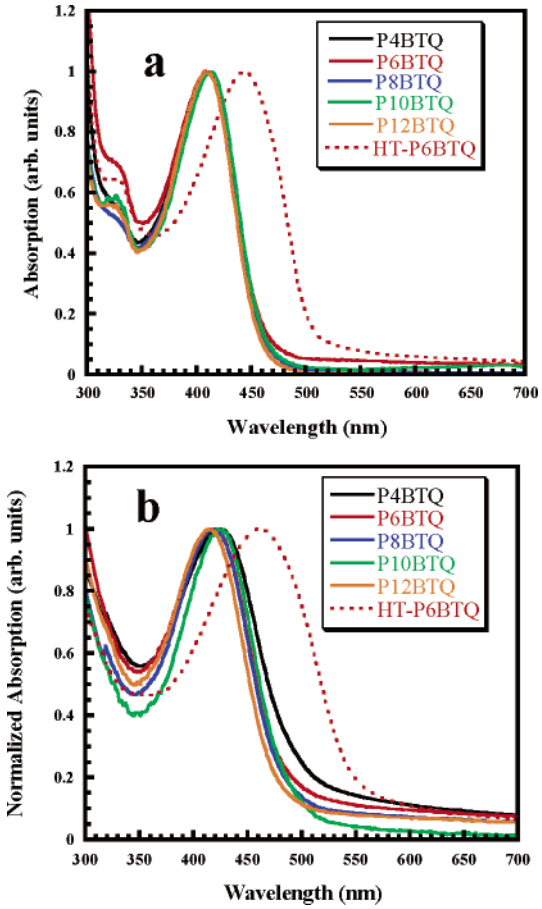

Figure 4. Optical absorption spectra of all polymers in THF solution (10^{-6} M) (a) and as thin films (b).

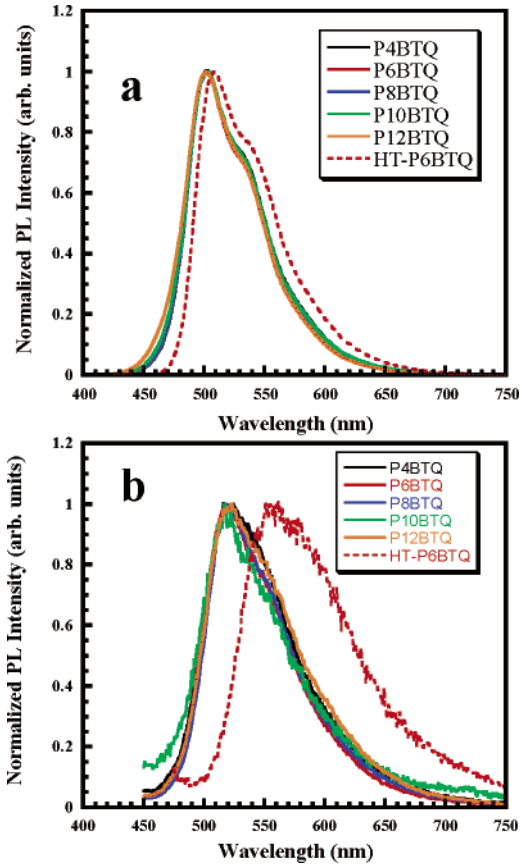

Figure 5. Photoluminescence (PL) spectra of all polymers in THF solution (10^{-6} M) (a) and as thin films (b). The excitation wavelength was 415 nm for PxBTQ (x = 4, 6, 8, 10, and 12) and 465 nm for HT-PGBTQ.

for P4BTQ to 2170 cd/m^2 for P6BTQ (Table 4). Peak performance was found in diodes using P6BTQ as the electron transport material, achieving a brightness of 2170 cd/m^2 and an external quantum efficiency of 1.4%. All the other HH-PxBTQs displayed EL device efficiencies between 0.86 and 1.0%. There is no discernible reason for the peak performance of P6BTQ. It is reasonable to assume that a smaller alkyl chain length may lead to smaller interchain distances, higher electron mobility, and balanced charge recombination. However, this is not supported by the poorer performance of P4BTQ relative to P6BTQ. One possible explanation for P6BTQ outperforming P4BTQ as an electron transport material is the much higher (∼4×) molecular weight (M_w) of P6BTQ compared to that of P4BTQ. Lower molecular weight materials have the possibility for more trapping sites at the functionalized chain ends. When HT-P6BTQ was used as the electron transport layer, the EL efficiency decreased to 0.29%, and there was a 2-fold increase in current. This is likely due to the decreased hole blocking ability of this polymer due to its small ionization potential (5.22 eV).

The weak-to-moderate intrinsic electroluminescence of the present series of polymers, their relatively high electron affinity (2.9−3.0 eV), their rather high glass transition temperature (∼160−250 °C), and their solubility in *both* aprotic organic solvents (chloroform, tetrahydrofuran, toluene, etc.) and formic acid make them very attractive for use as electron transport materials in organic LEDs. Solubility in formic acid and other protonic solvents facilitated their use in bilayer device architectures as demonstrated here. Solubility in aprotic organic solvents makes polymer blend devices possible as recently demonstrated for one of the new PxBTQ polymers (P8BTQ or POBTPQ).[10d] Although the electron transport properties of these series of polymers were explored here with only MEH−PPV, we believe that these new electron transport materials could be used with other emissive polymers including other arylenevinylene polymers, polyfluorenes, polyphenylenes, and polythiophenes.

Conclusions

We have synthesized a series of new soluble n-type conjugated polymers incorporating bis(phenylquinoline)

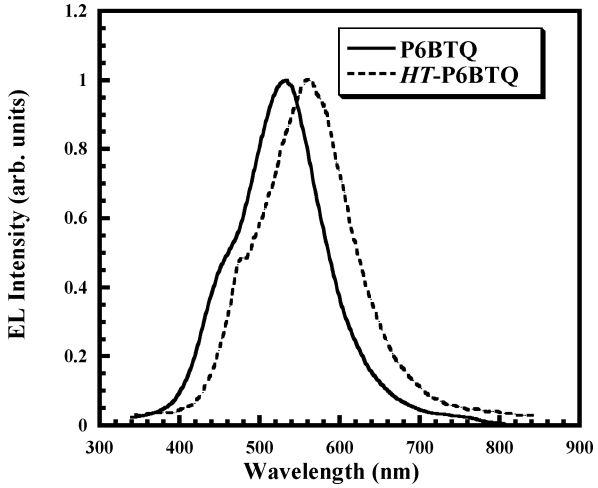

Figure 6. Normalized EL spectra of ITO/PEDOT/**Polymer**/Al diodes at an applied voltage of 13 V.

Table 3. EL Device Properties of New Polyquinolines as the Emissive Layer[a]

polymer	λ^{EL}_{max} (nm)	V_{on} (V)	I_{max} (A/cm^3)	L_{max} (cd/m^2)	EQE (%)
P4BTQ	538	10	333	16	0.004
P6BTQ	529	9	293	57	0.015
P8BTQ	530	9	348	64	0.015
P10BTQ	533	10	312	41	0.009
P12BTQ	538	10	282	38	0.010
HT-P6BTQ	562	9.5	331	21	0.004

[a] LEDs of the type ITO/PEDOT/polymer/Al.

and a regioregular dialkylbithiophene in the polymer backbone and investigated the electrochemical, photophysical, electroluminescent, and electron transport properties. The X-ray single-crystal structure of a model compound BPQ-10BT allowed quantification of the intramolecular torsion angle and the disordered nature of the alkyl chains in the head-to-head polymers (PxBTQs). The steric interaction between the alkyl chain and the neighboring thiophene unit results in a 45° torsion angle between the two thiophene rings, decreasing planarity and conjugation length. Cyclic voltammetry showed that the reduction of the polymers was quasi-reversible while the oxidation was irreversible. Estimated electron affinities (LUMO levels) of the new polymers were 2.88−2.97 eV, which together with their high T_gs (161−256 °C) suggested that they have promising electron transport properties for organic LEDs. Initial use of the polymers as the electron transport materials in bilayer MEH−PPV-based LEDs showed substantial enhancement in device performance under ambient air conditions (up to 1.4% external quantum efficiency and 2170 cd/m^2 luminance).

Experimental Section

Materials. 3-Alkylthiophenes were purchased from TCI, Inc. Diphenyl phosphate, *m*-cresol, 2-aminobenzophenone (**8**), and all other reagents and solvents were purchased from Aldrich and used as received.

Synthetic Procedures. Synthesis of **2c** and **6c** has been described elsewhere.[14a] 3,3′-Dibenzoylbenzidine (**5**),[16] the 3,3′-dialkyl-2,2′-bithiophenes (**1a**−**1e**),[15a,b] and 3,4′-dihexyl-2,2′-bithiophene (**3**)[15c] were synthesized according to literature methods.

General Procedure for Acetylation of 3,3′-Dialkyl-2,2′-bithiophene and 3,4′-Dihexyl-2,2′-bithiophene. To a stirred solution of the 3,3′-dialkyl-2,2′-bithiophene in 100 mL of dry CH_2Cl_2 was added a solution of acetic anhydride in dry CH_2Cl_2 (2.4 equiv) and a solution of $SnCl_4$ in dry MeCN (2.4 equiv). The resulting solution was refluxed for 24 h and then poured over crushed ice containing 50 mL of glacial acetic acid. The organic layer was collected, and the aqueous layer was extracted with CH_2Cl_2 (2 × 100 mL). The combined organic layers were washed with 10% NaOH solution, dried with $MgSO_4$, and concentrated. The product was purified on silica gel column (eluent 1:1 CH_2Cl_2:hexanes).

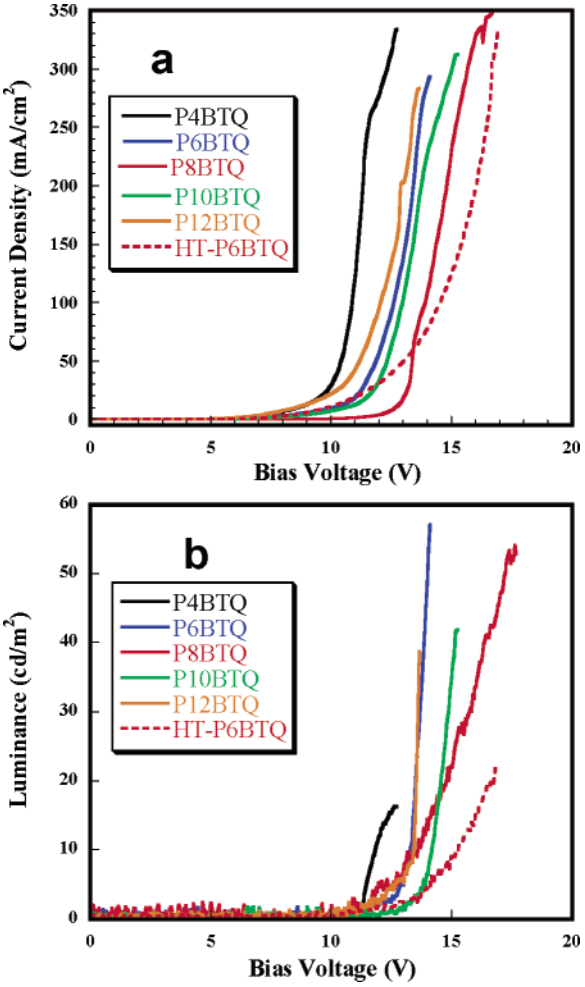

Figure 7. Voltage−current (a) and voltage−luminance (b) curves of ITO/PEDOT/PxBTQ/Al diodes.

5,5′-Diacetyl-3,3′-dibutyl-2,2′-bithiophene (2a). An amber liquid was recovered (1.1 g, 33%). ^{1}H NMR (499 MHz, $CDCl_3$, 298 K) δ (ppm): 7.53 (s, 2H); 2.58 (s, 6H); 2.55 (t, 4H); 1.58 (m, 4H); 1.26 (s, 4H); 0.89 (t, 6H). FT-IR (cm^{-1}): 2933, 2922, 2851, 1663, 1520, 1405, 1358, 1305, 1255, 867, 765. Calcd for $C_{20}H_{26}O_2S_2$: C, 66.26; H, 7.23; O, 8.83; S, 17.69. Found: C, 65.95; H, 6.98; S, 16.93.

5,5′-Diacetyl-3,3′-dihexyl-2,2′-bithiophene (2b). An amber liquid was recovered (2.1 g, 39%). ^{1}H NMR (499 MHz, $CDCl_3$, 298 K) δ (ppm): 7.57 (s, 2H); 2.56 (s, 6H); 2.53 (t, 4H); 1.55 (m, 4H); 1.24 (s, 12H); 0.84 (t, 6H). FT-IR (cm^{-1}): 2926, 2855, 1659, 1528, 1411, 1358, 1270, 909, 728. Calcd for $C_{24}H_{34}O_2S_2$: C, 68.85; H, 8.19; O, 7.64; S, 15.32. Found: C, 69.23; H, 8.54; S, 14.92.

5,5′-Diacetyl-3,3′-didecyl-2,2′-bithiophene (2d). An amber liquid was recovered (3.2 g, 41%). ^{1}H NMR (499 MHz, $CDCl_3$, 298 K) δ (ppm): 7.59 (s, 2H); 2.57 (s, 6H); 2.53 (t, 4H); 1.58 (m, 4H); 1.21 (s, 28H); 0.93 (t, 6H). FT-IR (cm^{-1}): 2955, 2933, 2851, 1663, 1411, 1351, 1275, 1205, 1002, 865, 615. Calcd for $C_{32}H_{50}O_2S_2$: C, 72.40; H, 9.49; O, 6.03; S, 12.08. Found: C, 72.07; H, 9.26; S, 11.63.

5,5′-Diacetyl-3,3′-didodecyl-2,2′-bithiophene (2e). An amber liquid was recovered (0.90 g, 37%). ^{1}H NMR (499 MHz, $CDCl_3$, 298 K) δ (ppm): 7.58 (s, 2H); 2.58 (s, 6H); 2.53 (t, 4H);

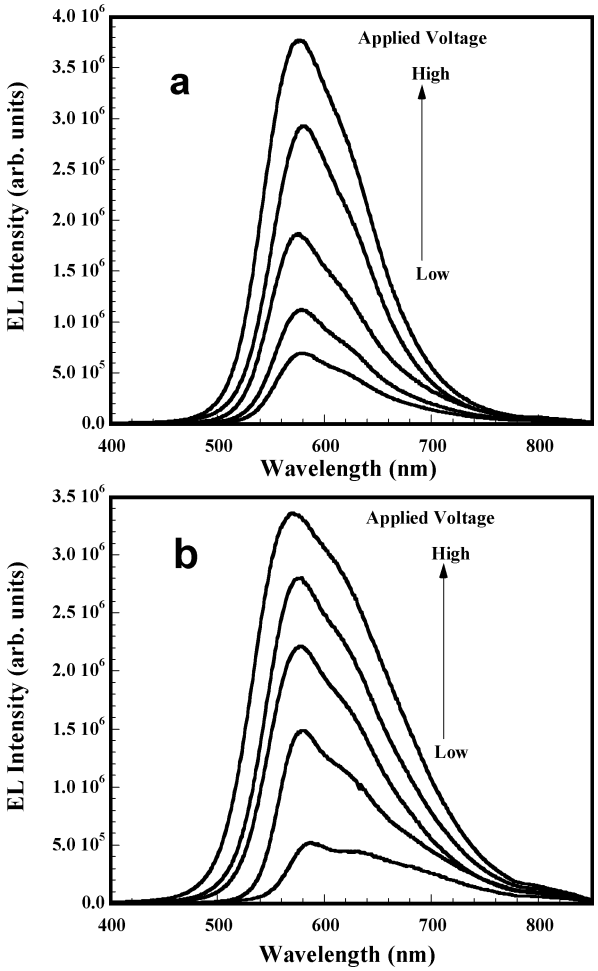

Figure 8. EL spectra of ITO/PEDOT/MEH−PPV/ P6BTQ /Al diode (a) and of ITO/PEDOT/ MEH−PPV/HT-P6BTQ /Al diode (b).

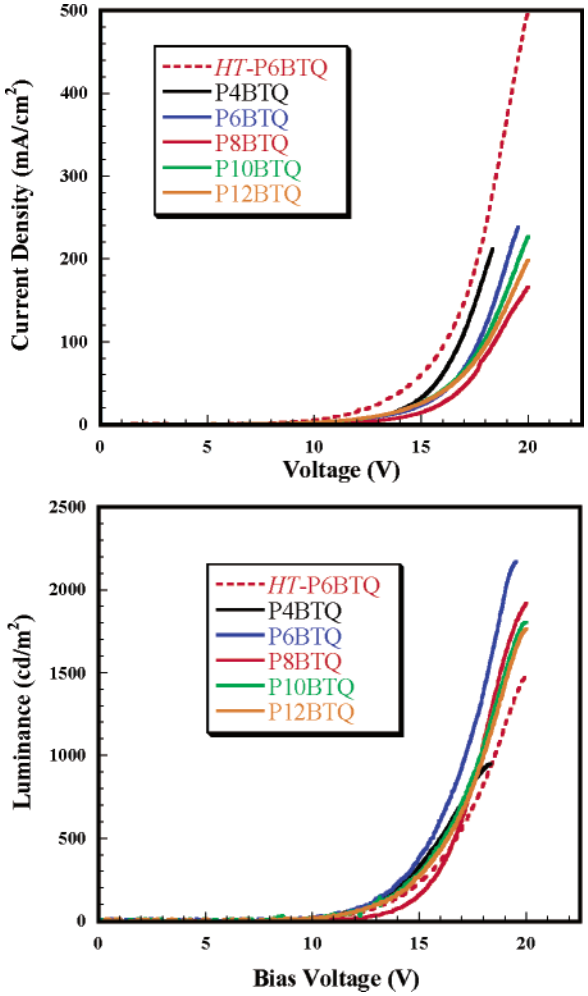

Figure 9. Voltage−current (a) and voltage−luminance curves (b) for ITO/PEDOT/MEH−PPV/PxBTQ/Al diodes.

1.57 (m, 4H); 1.25 (s, 36H); 0.89 (t, 6H). FT-IR (cm^{-1}): 2931, 2855, 1657, 1523, 1465, 1409, 1358, 1265, 1152, 1041, 919, 881, 775, 607. Calcd for $C_{36}H_{58}O_2S_2$: C, 73.66; H, 9.96; O, 5.45; S, 10.92. Found: C, 73.34; H, 9.72; S, 10.59.

5,5′-Diacetyl-3,4′-dihexyl-2,2′-bithiophene (4). An amber oil recovered (3.6 g, 49% yield). ^{1}H NMR (499 MHz, $CDCl_3$, 298 K) δ (ppm): 7.55 (s, 1H); 7.14 (s, 1H); 2.98 (t, 2H); 2.86 (t, 2H); 2.58 (s, 6H); 1.60 (m, 4H); 1.37 (s, 12H); 0.96 (t, 6H). FT-IR (cm^{-1}): 2926, 2855, 1659, 1528, 1411, 1358, 1270, 909, 728. Calcd for $C_{24}H_{34}O_2S_2$: C, 68.85; H, 8.19; O, 7.64; S, 15.32. Found: C, 69.22; H, 8.24; S, 14.81.

General Procedure for Polymerization. One equivalent (∼1 mmol) each of diacetyldialkylbithiophene and 3,3′-dibenzoylbenzidine, 10 g of diphenyl phosphate (DPP), and 5 g of *m*-cresol were added to a cylindrical reaction vessel. The reactor was purged with argon for 20 min. The mixture was mechanically stirred under static argon as the temperature was gradually increased to 140 °C over a period of 12 h. The polymerization mixture was stirred at this temperature for 72 h and then precipitated into 10% triethylamine/ethanol. The precipitate was collected by vacuum filtration and extracted on Soxhlet apparatus for 72 h with 20% triethylamine/ethanol. The polymer was then dissolved in $CHCl_3$ and precipitated into ethanol, collected by vacuum filtration, and then dried at 60 °C in a vacuum for 24 h.

Poly(2,2′-(3,3′-dibutyl-2,2′-bithienylene-6,6′-bis(4-phenylquinoline)) (P4BTQ). 3,3′-Dibenzoylbenzidine (484.4 mg, 1.24 mmol) and 3,3′-didecyl-5,5-diacetyl-2,2′-bithiophene (451.2 mg, 1.24 mmol) were used. 0.760 g (88%) of brown powder was recovered. ^{1}H NMR (499 MHz, $CDCl_3$, 298 K) δ (ppm): 8.22 (d, 2H); 8.11 (s, 2H); 8.01 (d, 2H); 7.78 (s, 2H); 7.71 (s, 2H); 7.60 (s, 10H); 2.67 (s, 4H); 1.66 (s, 4H); 1.28 (m, 36H); 0.85 (t, 6H). FT-IR (cm^{-1}): 2952, 2898, 1653, 1587, 1541, 1457, 1357, 1267, 1186, 1021, 926, 826, 766, 622. Calcd for $C_{46}H_{38}N_2S_2$: C, 80.90; H, 5.61; N, 4.10; S, 9.39. Found: C, 75.09; H, 5.43; N, 3.87; S, 7.15.

Table 4. LED Properties of Polyquinoline Electron Transport Layer

polymer	λ^{EL}_{max}	V_{on} (V)	I_{max} (A)	L_{max} (cd/m^2)	EQE (%)
P4BTQ	570	8.5	212	948	1.0
P6BTQ	569	8.0	239	2170	1.4
P8BTQ	570	9.0	166	1916	0.88
P10BTQ	572	9.0	227	1805	0.90
P12BTQ	571	8.5	199	1763	0.86
HT-P6BTQ	570	9.0	500	1476	0.29

[a] Polymers were in diodes of the type ITO/PEDOT/MEH−PPV/PxBTQ/Al.

Poly(2,2′-(3,3′-dihexyl-2,2′-bithienylene-6,6′-bis(4-phenylquinoline)) (P6BTQ). 3,3′-Dibenzoylbenzidine (536.1 mg, 1.36 mmol) and 3,3′-didecyl-5,5-diacetyl-2,2′-bithiophene (570.8 mg, 1.36 mmol) were used. 0.825 g (82%) of fibrous yellow solid was recovered. ^{1}H NMR (499 MHz, $CDCl_3$, 298 K) δ (ppm): 8.22 (d, 2H); 8.11 (s, 2H); 8.01 (d, 2H); 7.78 (s, 2H); 7.71 (s, 2H); 7.60 (s, 10H); 2.67 (s, 4H); 1.66 (s, 4H); 1.28 (m, 36H); 0.85 (t, 6H). FT-IR (cm^{-1}): 2924, 2854, 1653, 1558, 1541, 1457, 1357, 1227, 1194, 1041, 926, 852, 721, 667. Calcd for $C_{50}H_{46}N_2S_2$: C, 81.26; H, 6.27; N, 3.79; S, 8.68. Found: C, 73.32; H, 5.70; N, 3.87; S, 6.73.

Poly(2,2′-(3,3′-didecyl-2,2′-bithienylene-6,6′-bis(4-phenylquinoline)) (P10BTQ). 3,3′-Dibenzoylbenzidine (347.6 mg, 0.95 mmol) and 3,3′-didecyl-5,5-diacetyl-2,2′-bithiophene (506.5 mg, 0.95 mmol) were used. 0.620 g (76%) of fibrous

orange material was recovered. ^{1}H NMR (499 MHz, $CDCl_3$, 298 K) δ (ppm): 8.22 (d, 2H); 8.11 (s, 2H); 8.01 (d, 2H); 7.78 (s, 2H); 7.71 (s, 2H); 7.60 (s, 10H); 2.67 (s, 4H); 1.66 (s, 4H); 1.28 (m, 36H); 0.85 (t, 6H). FT-IR (cm^{-1}): 2920, 2902, 1585, 1544, 1456, 1421, 1022, 826, 699, 621. Calcd for $C_{58}H_{62}N_2S_2$: C, 81.83; H, 7.34; N, 3.29; S, 7.53. Found: C, 80.99; H, 6.95; N, 3.45; S, 6.23.

Poly(2,2′-(3,3′-didodecyl-2,2′-bithienylene-6,6′-bis(4-phenylquinoline)) (P12BTQ). 3,3′-Dibenzoylbenzidine (201.3 mg, 0.51 mmol) and 3,3′-didecyl-5,5-diacetyl-2,2′-bithiophene (301.1 mg, 0.51 mmol) were used. 0.362 g (76%) of brown powder was recovered. ^{1}H NMR (499 MHz, $CDCl_3$, 298 K) δ (ppm): 8.22 (d, 2H); 8.11 (s, 2H); 8.01 (d, 2H); 7.78 (s, 2H); 7.71 (s, 2H); 7.60 (s, 10H); 2.67 (s, 4H); 1.66 (s, 4H); 1.28 (m, 36H); 0.85 (t, 6H). FT-IR (cm^{-1}): 2920, 2850, 1586, 1536, 1461, 1421, 1068, 826, 700, 621. Calcd for $C_{62}H_{70}N_2S_2$: C, 82.07; H, 7.78; N, 3.09; S, 7.07. Found: C, 79.67; H, 7.83; N, 2.81; S, 6.95.

Poly(2,2′-(3,4′-dihexyl-2,2′-bithienylene-6,6′-bis(4-phenylquinoline)) (HT-P6BTQ). 3,3′-Dibenzoylbenzidine (441.5 mg, 1.13 mol) and 3,3′-didecyl-5,5-diacetyl-2,2′-bithiophene (471.4 mg, 1.13 mmol) were used. 0.620 g (74%) of red semifibrous material was recovered. ^{1}H NMR (499 MHz, $CDCl_3$, 298 K) δ (ppm): 8.22 (d, 2H); 8.03 (s, 2H); 7.98 (d, 2H); 7.70 (s, 2H); 7.68 (s, 1H); 7.60 (s, 10H); 7.11 (s, 1H); 2.66 (s, 4H); 1.63 (s, 4H); 1.25 (m, 36H); 0.82 (t, 6H). FT-IR (cm^{-1}): 2918, 2905, 1583, 1546, 1436, 1421, 1022, 826, 699, 621. Calcd for $C_{50}H_{46}N_2S_2$: C, 81.26; H, 6.27; N, 3.79; S, 8.68. Found: C, 76.45; H, 6.17; N, 3.85; S, 7.23.

2,2′-Bis(4-phenylquinoline)-3,3′-didecyl-2,2′-bithienylene (BPQ-10BT). 0.272 g of 5,5′-diacetyl-3,3′-didecyl-2,2′-bithiophene, 0.252 g of 2-aminobeznophenone, 1 g of diphenyl phosphate, and 5 mL of toluene were added to a flask. The flask was purged with argon for 20 min. The mixture was stirred under argon as temperature at 120 °C overnight. The mixture was then precipitated into 10% triethylamine/ethanol. The precipitate was collected by vacuum filtration and recrystallized twice from a 1:4 methanol/THF solution. 0.373 g of yellow oil was recovered (87% yield). T_m = 22 °C. ^{1}H NMR (499 MHz, $CDCl_3$, 298 K) δ (ppm): 8.19 (d, 2H); 7.88 (d, 2H); 7.71 (d, 2H); 7.60 (m, 10H); 7.46 (t, 2H); 7.37 (t, 2H); 7.06 (t, 2H); 2.69 (t, 4H); 1.70 (t, 4H) 1.35 (m, 28H); 0.99 (t, 6H). HRMS (FAB) calcd for $C_{58}H_{65}N_2S_2$ 853.458 77; found 853.458 85.

General. ^{1}H NMR and ^{13}C NMR spectra were recorded on a Bruker DRX-499 at 499 MHz using $CDCl_3$ as the solvent. Fourier transformation infrared (FT-IR) spectroscopy was done by using a Perkin-Elmer 1720 FT-IT spectrometer. The FTIR sample was a film on a KBr plate. Thermogravimetric analysis of the polymers was conducted on a TA Instruments Q50 TGA. A heating rate of 10 °C/min under flowing N_2 was used with runs being conducted from room temperature to 800 °C. Differential scanning calorimetry (DSC) was run on a TA Instruments Q100 DSC under flow of N_2. The heat−cool−heat method was used with an initial heating rate of 40 °C/min and a cooling rate of 20 °C/min and a final heating rate of 10 °C/min. All transitions were based upon the second heating. X-ray data were collected using a Nonius Kappa CCD utilizing Mo Kα radiation (λ = 0.710 73 Å).

Photophysics. Optical absorption spectra were obtained by using a Lambda-900 UV/vis/near-IR spectrophotometer (Perkin-Elmer). Steady-state photoluminescence (PL) studies were done by using a Photon Technology International Inc. (PTI) Instrument and a Xe lamp (75 W) as the excitation source in air at room temperature. In solution, the fluorescence quantum yield was determined using a perylene standard (87%).[25] A rough estimate of fluorescence quantum yield in the solid state was made by comparing the thin film of the polymer with a thin film of 9,10-diphenylanthracene in poly(methyl methacrylate) as a reference standard (83%).[26]

Cyclic Voltammetry. Cyclic voltammetry experiments were done on an EG&G Princeton Applied Research potentiostat/galvanostat (model 273A). Data were collected and analyzed by the model 270 Electrochemical Analysis System software. A three-electrode cell was used in all experiments as previously described.[20] Platinum wire electrodes were used as both counter and working electrodes, and silver/silver ion (Ag in 0.1 M $AgNO_3$ solution, Bioanalytical System, Inc.) was used as a reference electrode. The Ag/Ag^+ ($AgNO_3$) reference electrode was calibrated at the beginning of the experiments by running cyclic voltammetry on ferrocene as the internal standard in an identical cell without any polymer on the working electrode. By means of the internal ferrocenium/ferrocene (Fc^+/Fc) standard, the potential values, obtained in reference to Ag/Ag^+ electrode, were converted to the saturated calomel electrode (SCE) scale. The films of all polymers were coated on the Pt working electrode by dipping the Pt wire into the viscous solution in chloroform and then dried it in a vacuum oven at 80 °C for 8 h. An electrolyte solution of 0.1 M $TBAPF_6$ in acetonitrile was used in all experiments. All solutions in the three-electrode cell were purged with ultra-high-purity N_2 for 10−15 min before each experiment, and a blanket of N_2 was used during the experiment.

Fabrication and Characterization of LEDs. Two types of LEDs were fabricated and evaluated: ITO/PEDOT/PxBTQ/Al and ITO/PEDOT/MEH−PPV/PxBTQ/Al. Sequential spin-coating of the layers onto a cleaned ITO-coated glass substrate was used to fabricate the two types. A thin layer of poly(ethylenedioxythiophene)−poly(styrenesulfonate) (PEDOT) (~40 nm) was first spin-coated from its solution in water onto ITO and dried at 80 °C in a vacuum for 12 h. For ITO/PEDOT/PxBTQ/Al devices, thin films of the polyquinolines were spin-coated from 1.0 wt % solutions in $CHCl_3$ onto the PEDOT layer and dried at 80 °C in a vacuum for 10 h. In the case of ITO/PEDOT/MEH−PPV/PxBTQ/Al devices, the MEH−PPV thin film was spin-coated from a 0.5 wt % solution in $CHCl_3$ onto the PEDOT layer and dried at 50 °C in a vacuum for 10 h. The polyquinolines were then spin-coated from 0.5 wt % solutions in formic acid onto the MEH−PPV thin film. The multilayer thin films were dried in a vacuum at 80 °C for 10 h before deposition of the aluminum electrode under vacuum (3×10^{-6} Torr). A 100 nm thick aluminum layer was thermally deposited to form active diode areas of 0.2 cm^2 (5 mm diameter).

The film thickness was measured by using an Alpha step profilometer (model 500, KLA-Tencor, San Jose, CA), which has a resolution of ±1 nm. Electroluminescence (EL) spectra were measured on a Photon Technology International Inc. (PTI) Instrument. The electrical characteristics of the devices were measured on an HP4155A semiconductor parameter analyzer together with a Grasby S370 optometer equipped with a calibrated luminance sensor head. The EL quantum efficiencies of the diodes were measured by using the procedures similar to those previously reported.[10a] All fabrications and measurements were done under ambient laboratory conditions.

Acknowledgment. This research was supported by the U.S. Army Research Laboratory and the U.S. Army Research Office under Grant DAAD19-01-1-0676 and in part by the Office of Naval Research. The authors thank Jason Benedict for his assistance in obtaining the crystallographic information.

Supporting Information Available: Crystallographic data for BPQ-10BT, ^{1}H NMR spectra, TGA and DSC curves, cyclic voltammograms, and absorption and emission spectra. This material is available free of charge via the Internet at http://pubs.acs.org.

References and Notes

(1) Recent reviews on polymer electroluminescence: (a) Kraft, A.; Grimsdale, A. C.; Holmes, A. B. *Angew. Chem., Int. Ed.* **1998**, *37*, 402−428. (b) Heeger, A. J. *Solid State Commun.* **1998**, *107*, 673−679. (c) Bernius, M. T.; Inbasekaran, M.; O'Brien, J.; Wu, W. *Adv. Mater.* **2000**, *12*, 1737−1750. (d) Kim, D. Y.; Cho, H. N.; Kim, C. Y. *Prog. Polym. Sci.* **2000**, *25*, 1089−1139.

(2) (a) Neher, D. *Macromol. Rapid Commun.* **2001**, *22*, 1365−1385. (b) Redecker, M.; Bradley, D. D. C.; Inbasekaran, M.; Woo, E. P. *Appl. Phys. Lett.* **1998**, *73*, 1565−1567.

(3) (a) Hu, B.; Karasz, F. E. *J. Appl. Phys.* **2003**, *93*, 1995−2001. (b) Peng, Z.; Bao, Z.; Galvin, M. E. *Chem. Mater.* **1998**, *10*, 2086−2090. (c) Jenekhe, S. A.; Zhang, X.; Chen, X. L.; Choong, V.-E.; Gao, Y.; Hsieh, B. R. *Chem. Mater.* **1997**, *9*, 409−412. (d) Tarkka, R. M.; Zhang, X.; Jenekhe, S. A. *J. Am. Chem. Soc.* **1996**, *118*, 9438−9439. (e) Zhang, X.; Shetty, A. S.; Jenekhe, S. A. *Acta Polym.* **1998**, *49*, 52−55. (f) Zhang, X.; Shetty, A. S.; Jenekhe, S. A. *Macromolecules* **1999**, *32*, 7422−7429.

(4) (a) Yu, G.; Heeger, A. J. *J. Appl. Phys.* **1995**, *78*, 4510−4515. (b) Halls, J. J. M.; Walsh, C. A.; Greenham, N. C.; Marseglia, E. A. Friend, R. H.; Moratti, S. C.; Holmes, A. B. *Nature (London)* **1995**, *376*, 498−500. (c) Antoniadis, H.; Hsieh, B. R.; Abkowitz, M. A.; Jenekhe, S. A.; Stolka, M. *Synth. Met.* **1994**, *62*, 265−271. (d) Jenekhe, S. A.; Yi, S. *Appl. Phys. Lett.* **2000**, *77*, 2635−2637.

(5) (a) Bao, Z.; Dodabalapur, A.; Lovinger, A. J. *Appl. Phys. Lett.* **1996**, *69*, 4108−4110. (b) Sirringhaus, H.; Tessler, N.; Friend, R. H. *Science* **1998**, *280*, 1741−1744. (c) Babel, A.; Jenekhe, S. A. *Adv. Mater.* **2002**, *14*, 371−374. (d) Babel, A.; Jenekhe, S. A. *J. Phys. Chem. B* **2002**, *106*, 6129−6132. (e) Babel, A.; Jenekhe, S. A. *J. Am. Chem. Soc.* **2003**, *125*, 13656−13657.

(6) (a) Brown, A. R.; Bradley, D. D. C.; Burroughs, J. H.; Friend, R. H.; Greenham, N. C.; Burn, P. L.; Holmes, A. B.; Kraft, A. *Appl. Phys. Lett.* **1992**, *61*, 2793−2795. (b) Strukelj, M.; Papadimitrakopoulos, F.; Miller, T. M.; Rothberg, L. J. *Science* **1995**, *267*, 1969−1971.

(7) (a) Peng, Z.; Bao, Z.; Galvin, M. E. *Adv. Mater.* **1998**, *10*, 680−684. (b) Wang, C.; Jung, G. Y.; Hua, Y.; Pearson, C.; Bryce, M. R.; Petty, M. C.; Batsanov, A. S.; Goeta, A. E.; Howard, J. A. K. *Chem. Mater.* **2001**, *13*, 1167−1173. (c) Mikroyannidis, J. A.; Spiliopoulos, I. K.; Kasimis, T. S.; Kulkarni, A. P.; Jenekhe, S. A. *Macromolecules* **2003**, *36*, 9295−9302.

(8) He, Y.; Gong, S.; Hattori, R.; Kanicki, J. *Appl. Phys. Lett.* **1999**, *74*, 2265−2267.

(9) Alam, M. M.; Jenekhe, S. A. *Chem. Mater.* **2002**, *14*, 4775−4780.

(10) (a) Zhang, X.; Jenekhe, S. A. *Macromolecules* **2000**, *33*, 2069−2082. (b) Zhang, X.; Kale, D. M.; Jenekhe, S. A. *Macromolecules* **2002**, *35*, 382−393. (c) Zhu, Y.; Alam, M. M.; Jenekhe, S. A. *Macromolecules* **2003**, *36*, 8958−8968. (d) Alam, M. M.; Tonzola, C. J.; Jenekhe, S. A. *Macromolecules* **2003**, *36*, 6577−6587.

(11) (a) Cui, Y.; Zhang, X. Jenekhe, S. A. *Macromolecules* **1999**, *32*, 3824−3826. (b) Fukuda, T.; Yamamoto, T.; Ishikawa, K.; Takezoe, H.; Fukuda, A. *Appl. Phys. Lett.* **1996**, *68*, 2346−2348.

(12) (a) Agrawal, A. K.; Jenekhe, S. A. *Chem. Mater.* **1992**, *4*, 95−104. (b) Agrawal, A. K.; Jenekhe, S. A. *Macromolecules* **1993**, *26*, 895−905. (c) Agrawal, A. K.; Jenekhe, S. A. *Chem. Mater.* **1993**, *5*, 633−640.

(13) Agrawal, A. K.; Jenekhe, S. A.; Vanherzeele, H.; Meth, J. S. *J. Phys. Chem.* **1992**, *96*, 2837−2843.

(14) (a) Tonzola, C. J.; Alam, M. M.; Jenekhe, S. A. *Adv. Mater.* **2002**, *14*, 1086−1090. (b) Zhu, Y.; Alam, M. M.; Jenekhe, S. A. *Macromolecules* **2002**, *35*, 9844−9846. (c) Kim, J. L.; Kim, J. K.; Cho, H. N.; Kim, D. Y.; Kim, C. Y.; Hong, S. I. *Macromolecules* **2000**, *33*, 5880−5885. (d) Krüger, H.; Janietz, S.; Sainova, D.; Wedel, A. *Macromol. Chem. Phys.* **2003**, *204*, 1607−1615. (e) Zhan, X.; Liu, Y.; Wu, X.; Wang, S.; Zhu, D. *Macromolecules* **2002**, *35*, 2529−2537. (f) Chiang, C.-L.; Shu, C.-F. *Chem. Mater.* **2002**, *14*, 682−687.

(15) (a) Hoffman, K. J.; Carlsen, P. H. *Synth. Commun.* **1999**, *29*, 1607−1610. (b) Hoffman, K. J.; Bakken, E.; Samuelsen, E. J.; Carlsen, P. H. *Synth. Met.* **2000**, *113*, 39−44. (c) Li, W.; Maddux, T.; Yu, L. *Macromolecules* **1996**, *29*, 7329−7334.

(16) Pelter, M. W.; Stille, J. K. *Macromolecules* **1990**, *23*, 2418−2422.

(17) Stille, J. K. *Macromolecules* **1981**, *14*, 870−880.

(18) Shetty, A. S.; Liu, E. B.; Lachicotte, R. J.; Jenekhe, S. A. *Chem. Mater.* **1999**, *11*, 2292−2295.

(19) Tonzola, C. J.; Alam, M. M.; Kaminsky, W.; Jenekhe, S. A. *J. Am. Chem. Soc.* **2003**, *125*, 13548−13558.

(20) Agrawal, A. K.; Jenekhe, S. A. *Chem. Mater.* **1996**, *8*, 579−589.

(21) Jenekhe, S. A.; Lu, L.; Alam, M. M. *Macromolecules* **2001**, *34*, 7315−7324.

(22) Fungo, F.; Jenekhe, S. A.; Bard, A. J. *Chem. Mater.* **2003**, *15*, 1264−1272.

(23) Stuve, E. M.; Krasnopoler, A.; Sauer, D. E. *Surf. Sci.* **1995**, *335*, 177−185.

(24) (a) Jenekhe, S. A.; Osaheni, J. A. *Science* **1994**, *265*, 765−768. (b) Osaheni, J. A.; Jenekhe, S. A. *Macromolecules* **1994**, *27*, 739−742.

(25) Kavarnos, G. J.; Turro, N. J. *Chem. Rev.* **1986**, *86*, 401−409.

(26) Guilbault, G. G., Ed. *Practical Fluorescence*; Marcel Dekker: New York, 1990.

MA035971O